BER the international journal of bridge engineering management and research

A Methodology for Deriving a Probabilistic Braking Force Model from Traffic Data

Amirmahmoud Behzadi[1,*]; Simone Celati[2]; Michele D'Amato[1]; Agnese Natali[2]; and Walter Salvatore[2]

Submitted: 27 February 2025 **Accepted:** 30 March 2025 **Publication date:** 10 April 2025

DOI: 10.70465/ber.v2i2.28

Abstract: This study presents a methodology for deriving a probabilistic model for estimating the braking force, which, on the contrary, is traditionally based on deterministic approaches in bridge design codes. The stochastic model utilizes the weight-in-motion dataset collected from a provincial road bridge for observing real traffic load probabilistic distributions in terms of vehicle gross weight, vehicle length, and inter-vehicle distance. Using Monte Carlo simulations, traffic convoys are generated for calculating the resultant braking force by assuming deceleration profiles available in literature and different scenarios to account for various braking combinations among the vehicles within a convoy. Starting from the obtained empirical cumulative distribution function, the probabilistic model provides the resultant braking force associated with a given return period, incorporating dynamic amplification factors as well.

Comparisons are made to highlight that, within the span lengths investigated, the probabilistic model proposed provides higher resultant braking forces than those given by the deterministic model adopted by the Eurocode and the Italian Standards in cases of high return periods and low nominal lives (i.e., in cases of high no-occurrence probability). Conversely, values in agreement with or lower than those calculated using the deterministic models considered are obtained in other cases. Finally, some simplified design equations for the resultant braking forces are proposed for three different nominal lives, which are useful for assessing existing bridges or designing new ones.

Author keywords: Braking force; traffic data; WIM data; probabilistic approach; Monte Carlo simulation

Introduction

Braking forces are horizontal loads that must be properly considered when designing new bridges or assessing existing ones, as explicitly specified in many standards, such as Eurocodes (EC0[1] and EC1-2[2]) and AASHTO LRFD Bridge Design Specifications.[3] Traditionally, they are calculated using deterministic approaches, relying on reference traffic scenarios where the number and types of vehicles are assumed, as specified, for instance, in Eurocodes (EC0[1] and EC1-2[2]), Italian standards,[4] Swiss standards (SIA 160[5] and SIA 261[6]), and British Standard BS 5400.[7]

However, it is recognized that for new or existing structures, such as bridges, probabilistic models for loads, including braking ones, are required. These models are needed within the probabilistic-based procedures adopted by many design standards. For instance, in EC1-2,[2] as *Load Model 1* (*LM1*) and *Load Model 2*, the vertical traffic load characteristic value is associated with a 1000-year return period (equivalent to a 5% exceedance probability in 50 years).

Recent advancements in traffic modeling have aimed to estimate braking forces using probabilistic approaches. These methods incorporate variability in key factors, such as vehicle characteristics, traffic dynamics, and driver behavior. By employing distributions derived from real traffic data, these approaches offer a more realistic representation of braking forces. Martins et al.[8] introduced a stochastic model incorporating traffic microsimulation tools to calculate the characteristic value of braking forces. Using realistic traffic scenarios from Swiss motorways and driver behavior data, they demonstrated that this probabilistic approach produces lower braking force values than those prescribed by design standards, while maintaining a safety target corresponding to a 1000-year return period. Additionally, Martins et al.[9] compared deterministic and probabilistic methodologies for deriving braking force load models. Their analysis revealed braking force values consistent with the same return period as vertical load models, factoring in the probability of a braking event occurring on a bridge. Breveglieri and Feltrin[10] developed a model integrating traffic data, stochastic variables, and bridge-specific properties to estimate braking forces. Their results emphasize the significant impact of bridge length, vehicle clustering, and braking event frequency on braking force magnitudes, making the model

*Corresponding Author: Amirmahmoud Behzadi.
Email: amirmahmoud.behzadi@unibas.it
[1]Department for Humanistic, Scientific, and Social Innovation (DIUSS), University of Basilicata, Italy
[2]Department of Civil and Industrial Engineering, School of Engineering, University of Pisa, Italy

Discussion period open till six months from the publication date. Please submit separate discussion for each individual paper. This paper is a part of the Vol. 2 of the International Journal of Bridge Engineering, Management and Research (© BER), ISSN 3065-0569.

an essential tool for design and performance assessment. Feltrin and Breveglieri[11] investigated the dynamic response of bridges to hard braking by trucks. Experimental results revealed that the bridge exhibited a nonlinear and more rigid behavior than expected based on the bearing properties. Their study concluded that a *single degree of freedom* (*SDOF*) model accurately represents bridge behavior during braking, particularly in capturing distinct longitudinal and vertical responses. Marshal et al.[12] conducted static and dynamic field tests to study the load path and intensity of braking force in highway shorter-span bridge substructures. The study revealed that the abutment is subjected to a maximum of roughly 75% of the braking force, while an individual column bent experiences up to 35%. The demand for each component is largely influenced by the location of the braking force and the relative stiffness of the component.

To date, probabilistic frameworks may be developed starting from detailed datasets obtained using *weigh-in-motion* (*WIM*) systems. These systems use advanced sensors to capture axle and gross vehicle weights, axle spacing, and vehicle speeds in real-time, facilitating continuous traffic monitoring and enabling detailed analyses of vehicle configurations and traffic flow. Furthermore, from a *WIM* dataset, it is possible to classify vehicles based on their type and configuration, enabling detailed traffic analyses and infrastructure load assessments. In recent years, *WIM* data have become increasingly vital for the probabilistic assessment of traffic loads, particularly in bridge design, maintenance, and safety evaluations. Many studies have used traffic microsimulation derived from *WIM* data to assess bridge load effects. Among others, Caprani[13] calibrated a traffic load model for short- to medium-length bridges using congested traffic microsimulation. Other traffic investigations based on *WIM* data analysis may be found in References.[14–17]

However, it should be noted that all works available to date in the literature focus on using *WIM* traffic data to monitor and analyze the vertical component of traffic action. Only recently have *WIM* data been considered as a useful tool for deriving braking forces. In Martins et al.,[8] *WIM* data gathered on Switzerland roads were used to estimate the braking force characteristic value. In this study, it was recognized that in modern standards, if simplified vehicle configurations are used, the braking force may be too conservative without a return period measure and inconsistent with the vertical load model. Recently, the vehicle–bridge interaction has gained attention from researchers. For example, Aloisio et al.[18] assessed vehicle–bridge interaction under braking through numerical simulations, surrogate modeling via machine learning, and experimental validation. Wang et al.[19] conducted a vehicle–bridge coupled vibration analysis to assess how braking affects mid-span displacement and impact factors in simply supported beam bridges. Through structural health monitoring and numerical modeling, Zhang et al.[20] examined the static and dynamic behavior of a semi-integral high-speed railway bridge under braking and high-speed traffic loads, highlighting the impact of structural flexibility and stiffness.

This paper proposes a methodology for deriving a *probabilistic braking force model* (*PBFM*) based on traffic data collected from *WIM* sensors installed to monitor a section before a bridge serving a provincial state road. Starting from *WIM* data, *probability density functions* (*PDFs*) of several parameters are derived, such as gross vehicle mass, length, and inter-vehicle distance. Then, using Monte Carlo simulations, vehicle convoys are randomly generated according to three different scenarios to calculate the maximum value of the resultant braking force. Since no information about vehicle deceleration profiles is available in the WIM data, this study applies the dataset from the 100-Car Naturalistic Driving Study (NDS)[21]. The proposed methodology permits the derivation of a *PBFM* capable of providing a resultant braking force dependent on the return period (or an exceedance probability in a given nominal life) and bridge span length, calculated using an *empirical cumulative distribution function* (*ECDF*) obtained through the stochastic methodology. In this study, the *PBFM* is proposed for bridge span lengths up to 50 m, as longer spans are uncommon for provincial roads.

Initially, a state-of-the-art review of some *deterministic braking force models* (*DBFMs*) is introduced, and the models recalled are examined in detail. Then, the proposed methodology is presented and applied to derive the *PBFM*, also incorporating dynamic amplification factors (DAFs) as proposed in the EC1-2 background document[22]. Comparisons with the *DBFM* adopted by EC1-2[2] and Italian standards[4] are shown and discussed. Finally, simplified design equations for the PBFM are derived for three different nominal lives (5, 30, and 50 years), which are useful for assessing existing bridges or designing new ones.

State of the Art

To date, several braking force models have been proposed in different design standards. These models primarily rely on deterministic assumptions about vehicle configurations, traffic loads, and braking behaviors.

SIA 160[5] originally adopted a braking force model based on experimental data collected from a series of tests on vehicle convoys. The model considered factors such as vehicle weight, initial speed, and deceleration, assuming a maximum braking force of 300 kN. According to this model, the maximum braking force transmitted to the pavement, $F_{b\,max}$, may be calculated using Newton's laws of motion as follows:

$$F_{b\,max} = max_t\{\sum_{i=1}^{N} m_i a_i\,(t)\} \tag{1}$$

In Eq. (1), m_i represents each vehicle's mass, N denotes the total number of vehicles, and $a_i(t)$ corresponds to the ith vehicle's time-dependent deceleration.

Later, in 2003, the SIA 261[6] proposed a braking force model for new bridges, based on the EC 1-2[2] model. This standard provides a maximum braking force of 900 kN for new bridges longer than 200 m.

In contrast, in 2011, SIA 269/1[6] reduced the maximum braking force to 600 kN in the case of existing bridges.

The British Standard BS 5400[7] introduced a more severe braking force model, which was particularly impactful for medium-length bridges. This model is based on shorter inter-vehicle distances, leading to frequent hard braking events with higher braking forces. Moreover, vehicle weights ranging from 16 to 32 tons and decelerations between 0.5 and 0.75 g were considered, making it more severe than other European codes. According to this model, the nominal load for normal traffic conditions (indicated as *HA*) ranges from 200 kN to a maximum of 700 kN.

Both Eurocode EC1-2[2] and Italian Standards NTC-2018[4] report the same formulation for deriving the resultant braking force. As clarified in the EC1-2 background document,[22] this formulation was proposed from a deterministic approach. The resultant braking force is associated with up to five vehicles, having a maximum assumed lorry weight of 40 tons and traveling at the same speed of 81 km/h, braking simultaneously with a deceleration of 0.5 g. This *DBFM* incorporates the *SDOF* dynamic effects, with *DAFs* depending on the number of vehicles. The braking force characteristic value Q_{1k}, limited to 900 kN, is calculated as a fraction of the vertical loads corresponding to *LM1* applied on *Lane 1*, according to the formulation:

$$Q_{1k} = 0.6\alpha_{Q1}\,(2Q_{1k}) + 0.1\alpha_{q1} q_{1k} w_1 \tag{2}$$

with the following limitation: $180\alpha_{Q1}\mathrm{kN} \leq Q_{1k} \leq 900\,\mathrm{kN}$, where Q_{1k} and q_{1k} are the axle loads and the uniformly distributed load of *LM1* for Lane 1, respectively. In this equation, w_1 indicates the wide lane, and L is attributed to the loaded length.

Fig. 1 compares the braking force characteristic value Q_{1k} computed according to the EC1-2[2] formulation (Eq. (2)) with the values obtained for convoys of up to five vehicles, each having a gross mass of 25, 30, and 40 tons.[22]

Finally, for the sake of completeness, Fig. 2 plots a comparison among the braking force models discussed in this section. As one may note, braking force models differ significantly across standards essentially due to varying assumptions and methodologies adopted. EC1-2[2] and NTC-2018[4] models are derived for heavy vehicles (HVs), such as 40-ton lorries, taking into account the bridge's dynamic response as well. In contrast, Swiss standards take a different approach: SIA 160[5] (1970) reaches a constant braking force of 300 kN, whereas in the case of SIA 261/1[6] (2011), a maximum value of 600 kN is provided for bridges over 100 m

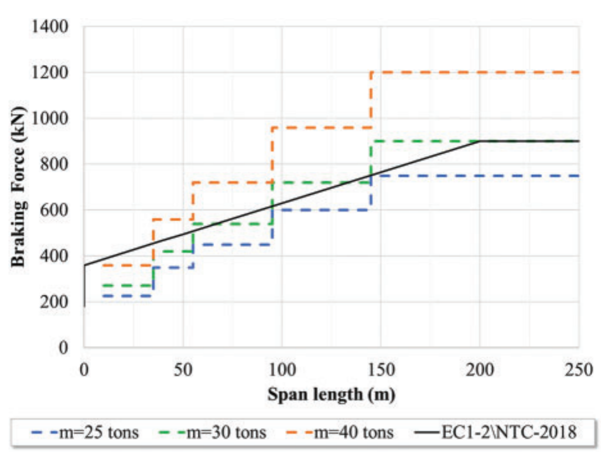

Figure 1. Braking force formulation proposed in EC1-2[2]

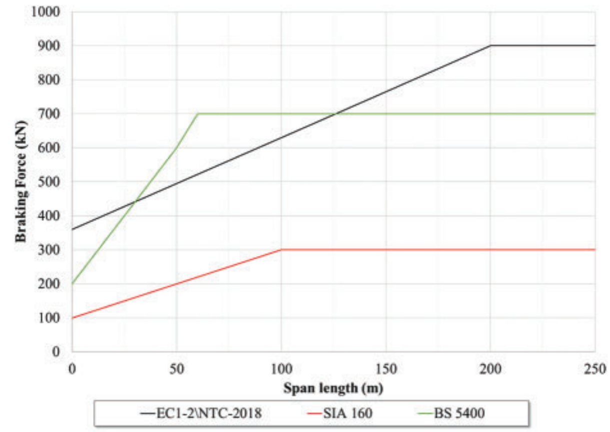

Figure 2. Comparison of braking force models

in length. Moreover, unlike other models that assume maximum simultaneous braking by all vehicles, these documents consider braking force as dependent on vehicle decelerations over time. Finally, as for BS 5400,[7] the braking force model provides higher braking forces than the EC1-2[2] model for medium span lengths, since shorter inter-vehicle distances are considered, leading to more frequent hard braking events and, consequently, higher estimated braking forces.

Descriptive Statistics

Nowadays, many design standard procedures are probabilistic-based, requiring that the braking force model is consistent with this approach to properly estimate traffic actions. Consequently, a probabilistic model capable of estimating the braking force is needed. Such a model would allow for the consideration of various return periods (T_R) or a given exceedance probability (p) within a specified nominal life (V_N), tailoring it to different design and assessment scenarios. For instance, a *PBFM* becomes particularly useful in the case of existing bridges, where the structural assessment may be conducted within a nominal life that may be significantly lower than the one considered for designing new bridges.

The methodology proposed in this study for deriving a *PBFM* is based on the analysis of *WIM* traffic data, assumed to be representative of the vertical traffic load passing over a bridge serving a certain road. In this case, *WIM* data from a provincial road are analyzed to derive probability distributions to define the vertical loads to be used in Monte Carlo simulations. Morespecifically, the following traffic data are analyzed: axle weight, vehicle length, axle number and spacing, and inter-vehicle distance, the latter defined as the interval distance between two consecutive vehicles. After analyzing the traffic data, vehicles are classified based on spacing and axle number. This study considers 12 vehicle categories, as illustrated in Table 1, where the axle number and their configuration are also reported. They vary from *Cat. A* having n. 2 axles to *Cat. N* with an axle number equal to or greater than 7. Figs. 3 and 4 illustrate the distribution of vehicle weight, length, and axle number across the n. 12

Table 1. Vehicle categories assumed

Category	No. of axles	Vehicle axle configuration
Cat. A	2	(O——O)
Cat. B	3	(O——O + —O—)
Cat. C	3	(O—-OO)
Cat. D	4	(O——O + ——OO)
Cat. E	4	n. 4 axles not belonging to Cat. D
Cat. F	5	(O——O + –OOO)
Cat. G	5	(O—-OO + O——O)
Cat. H	5	(O—-O–+–O—OO)
Cat. I	5	n. 5 axles not belonging to Cat. F, G, and H
Cat. L	6	(O—-O + —-OOOO)
Cat. M	6	n. 6 axles not belonging to Cat. L
Cat. N	≥7	At least 7 axles

vehicle categories considered. The box covers the interquartile range (Q1–Q3) with a 1.5 threshold applied to identify outliers, which are shown as red plus signs.

Then, WIM data are used to determine, for each category the frequency of occurrence and the *PDFs* of vehicle gross mass, vehicle length, and inter-vehicle distance. All data are processed using MATLAB®'s[23] and preliminarily cleaned to remove outliers, such as records with zero weight or unrealistically long vehicle lengths. As an example, Fig. 5 presents the resulting histogram and PDFs for vehicles belonging to Cat. B (Table 1). Specifically, Figs. 5a, 5b plot the histogram and the PDF of gross weight and vehicle length for Cat. B, respectively, where a Gaussian mixture distribution (GMD) is fitted to both histograms. Fig. 6 also indicates the histogram and exponential PDFs fitted to the inter-vehicle distance. This distribution is considered in this study as it ensures an accurate fit to the empirical data, particularly where multiple modes exist. The use of extreme value distributions, such as Gumbel, Weibull, and generalized extreme value, will be investigated in the future, as their application is beyond the scope of the current study. Histograms and PDFs for gross weight and length of all vehicle categories may be found in Appendix A and Appendix B, respectively. The analytical expressions for these distributions are derived from the fitted PDFs, which were estimated using MATLAB's *fitgmdist* function.

A crucial role in this methodology is played by the deceleration profile of each braking vehicle belonging to a certain convoy. In this work, the data from the 100-Car NDS,[21] the only freely accessible dataset regarding braking events, are considered for deriving the *PDF* of the maximum deceleration of each vehicle during a braking event. In particular, in this study,[21] 100 instrumented *light vehicles* (*LVs*) were monitored over approximately 1 year, with the aim of collecting driving data from instrumented vehicles, where drivers were given no special instructions. The database collected many extreme cases of driving, such as crashes, near-crashes, and other incidents, including data about speed, vehicle headway, time-to-collision, and driver reaction time. More details about this study may be found elsewhere.[21] As for *HVs*, the dataset created by Martins et al.[24] is considered in this work. This dataset was developed using supplementary data derived from the 100-Car NDS and adjusted to account for *HV*-specific characteristics. Similarly to the LVs, a *PDF* of the maximum deceleration of each vehicle during the braking event is derived for the HVs. Afterwards, it is assumed that the *PDF* derived for the maximum deceleration of the *LVs* is assigned to Cat. A vehicles, while the *PDF* derived for the maximum deceleration of the *HVs* is assigned to vehicles from Cat. B to Cat. N vehicles. Fig. 7 illustrates the histograms and the derived PDFs for the maximum deceleration of *LVs* and *HVs*, where a *GMD* is fitted for both. In particular, Fig. 7a refers to *HVs*, reaching a maximum deceleration value of up to 7 m/sec,[2] while Fig. 7b pertains to *LVs*, reaching a maximum value of 12 m/sec^2. Subsequently, a generalized Pareto distribution is assumed

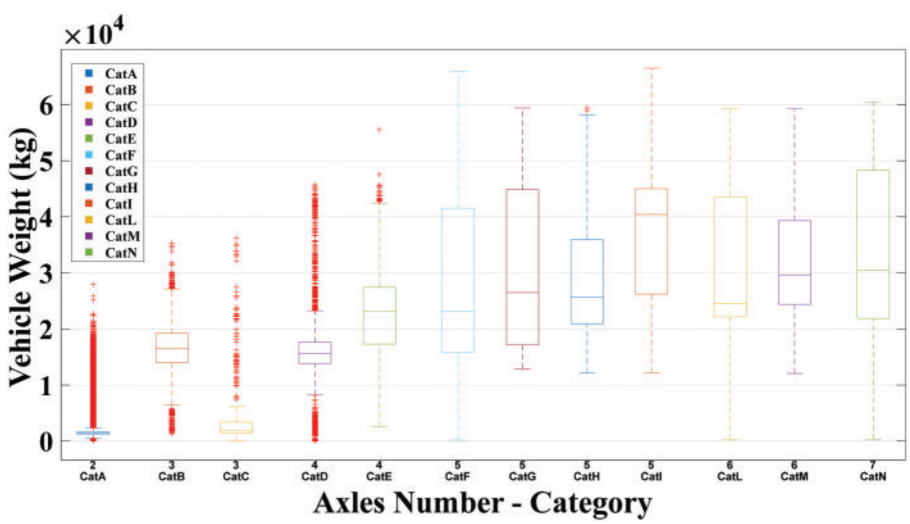

Figure 3. Boxplot of vehicle weight by axle number

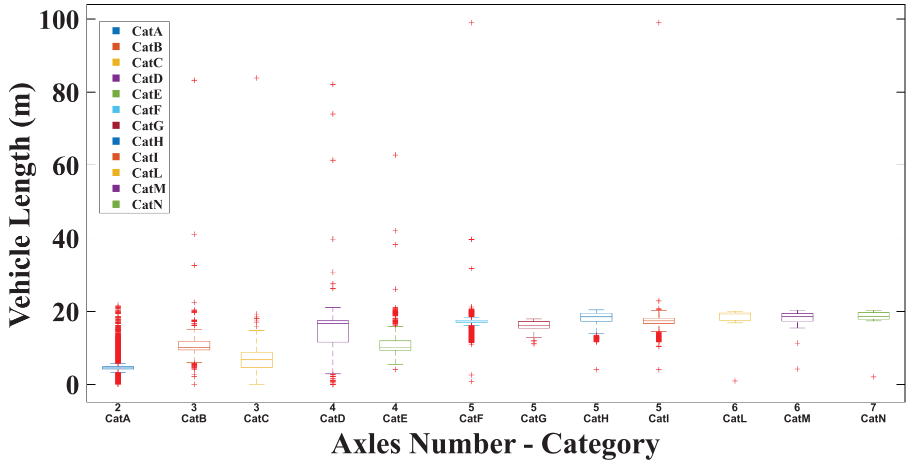

Figure 4. Boxplot of vehicle length by axle number

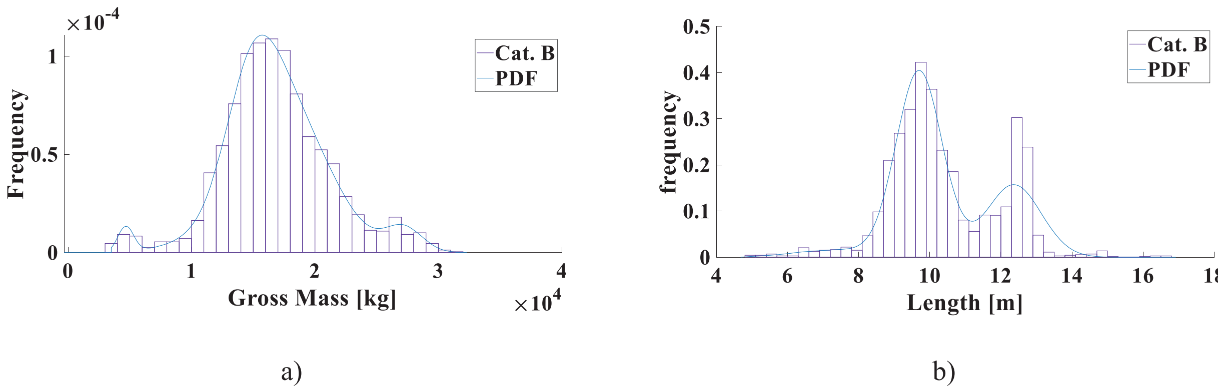

Figure 5. Histogram and PDF of (a) vehicle gross mass and (b) vehicle length

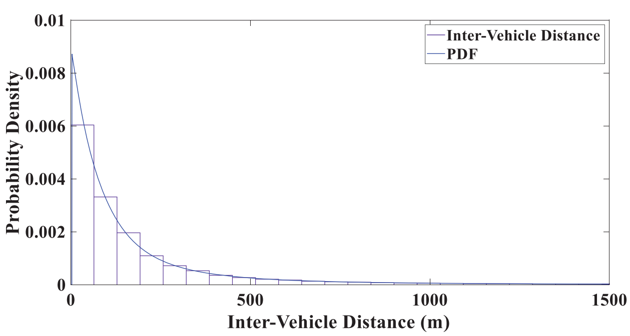

Figure 6. The mixture of three exponential PDFs fitted to the inter-vehicle distance

for hard braking events (deceleration equal to or higher than 4 m/s^2).

Methodology Proposed for Deriving a PBFM

For each span length, several convoy configurations are generated with an increasing number of vehicles, starting from the configuration containing only one vehicle. Initially, for each convoy configuration, a Monte Carlo simulation is implemented to randomly sample the vehicle category according to the classification reported in Table 1. After sampling the category, a nested Monte Carlo simulation with 10^7 extractions is performed for each vehicle. In each extraction, gross mass, length, inter-vehicle distance, and deceleration are extracted from the corresponding *PDFs* and assigned to the corresponding vehicle. The proposed methodology is illustrated as a flowchart in Fig. 8.

In the proposed *PBFM*, each convoy is associated with a braking event. For the generic convoy (Fig. 9) made up of *n* vehicles (belonging to the 12 categories of Table 1), the resultant braking force F_{bf} (Eq. (3)) is calculated as follows:

$$F_{bf} = \sum\nolimits_{i=1}^{n} f_{bf,i} = \sum\nolimits_{i=1}^{n} m_i \cdot a_i \tag{3}$$

where $f_{bf,i}$, m_i, and a_i are the braking force, gross mass, and deceleration value of the *i*th vehicle, respectively. It should be noted that the resultant braking force F_{bf} is subjected to the constraint that the convoy's total length L_c (Eq. (4)) does not exceed the bridge span length L (Fig. 9). L_c may be calculated as follows:

$$L_c = \sum\nolimits_{i=1}^{n} l_i + \sum\nolimits_{j=1}^{n-1} IVD_j \tag{4}$$

where l_i is the vehicle length, and IVD_j is the inter-vehicle distance between the *i*th and (*i-1*)th vehicle (i.e., the previous vehicle).

For each bridge span length L, Monte Carlo simulations permit the derivation of a sample of braking force values (sorted in ascending order) $\{F_{bf1}, F_{bf2}, \ldots, F_{bfm}\}_L$.

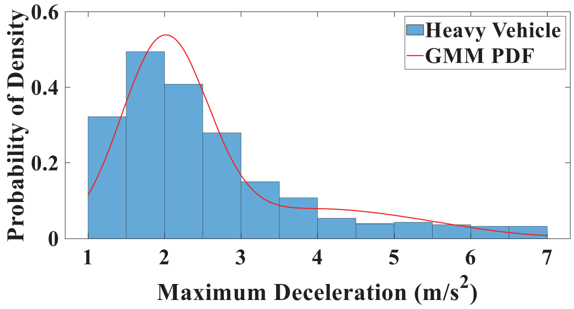

a)

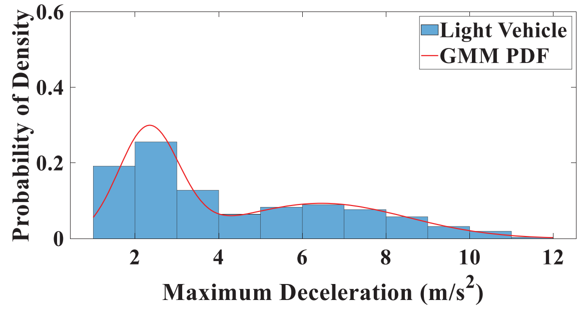

b)

Figure 7. Histogram and PDF of the maximum deceleration of: (a) HV and (b) LV

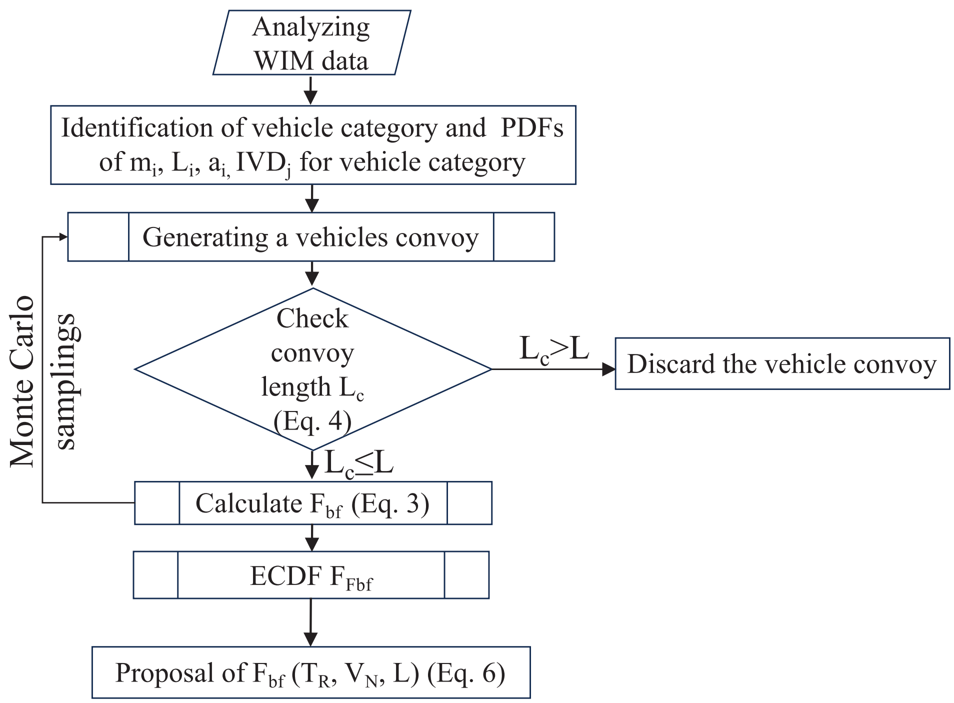

Figure 8. Flowchart of the proposed methodology

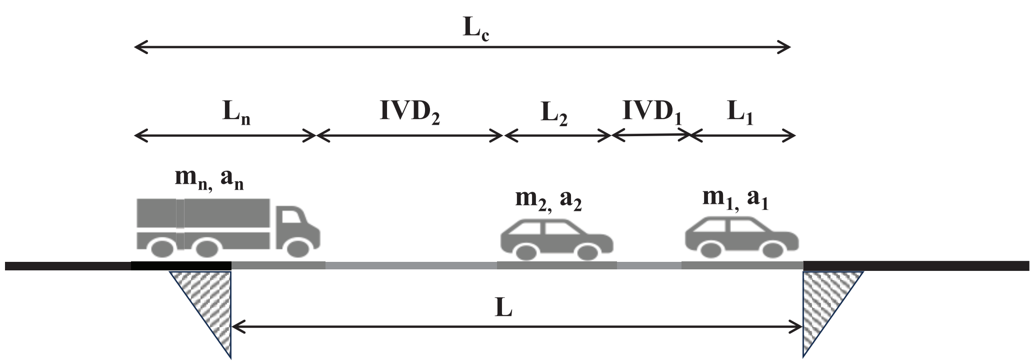

Figure 9. Example of convoy for a braking event

This is done by randomly sampling the vehicle category and then the gross vehicle mass, length, and inter-vehicle distance from their corresponding *PDFs* defined earlier. Consequently, an *ECDF* is derived $F_{F_{bf,L}}$, representing the cumulative distribution of the resultant braking forces thus obtained. $F_{F_{bf,L}}$ is consistent with specific *WIM* traffic data, assumed to be representative of the vertical traffic load of a given road.

The *PBFM* is based on the assumption that $p = F_{F_{bf,L}}(q)$ is the probability of no-occurrence referred to the quantile of order q (q-quantile). Therefore, $1 - p$ corresponds to the occurrence probability of a braking force with a value equal to q. The no-occurrence probability p of a braking force with a value q, having a return period T_R within a bridge nominal life V_N is given as

$$p = \left(1 - \frac{1}{T_R}\right)^{V_N} \tag{5}$$

Table 2 indicates the probability of no-occurrence p corresponding to the given return period T_R and nominal life V_N.

In this research, a vehicle convoy is considered to be involved in a braking event when at least one vehicle experiences a deceleration equal to or higher than 4 m/s^2. This threshold is used, for instance, in Martins et al.[24], to define a hard braking event. This study disregards potential collisions or skidding among vehicles, providing a conservative estimate of the resultant braking force. Moreover, three scenarios are defined to evaluate the braking force during a braking event:

Scenario 1 considers convoys made up of any vehicle categories, including Cat. A (with the *PDF* for the maximum deceleration of *LVs* assigned) and Cat. B to N (with the *PDF*

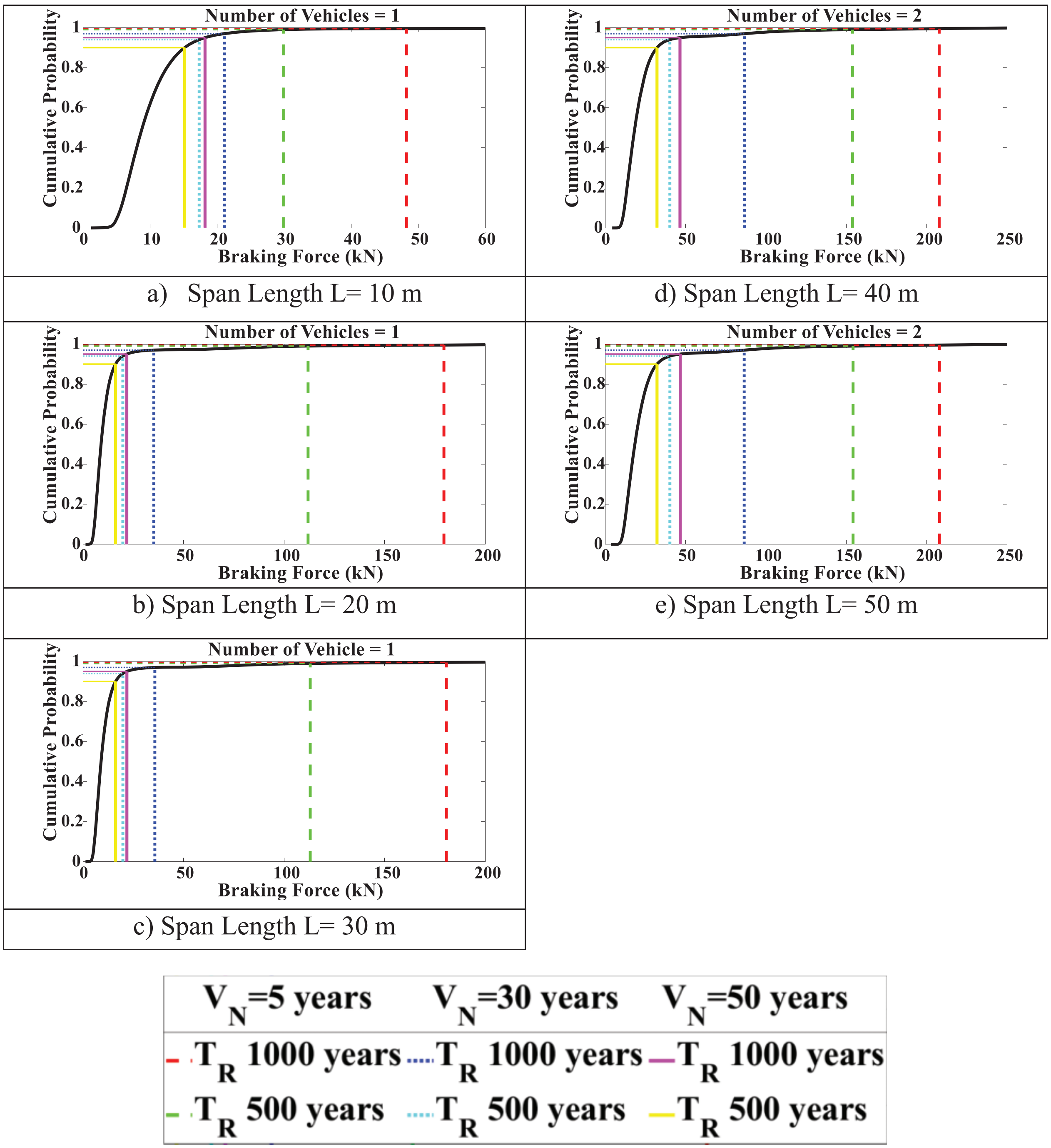

Figure 10. Scenario 1: ECDFs for several span lengths

for the maximum deceleration of *HVs* assigned) (Table 1). All convoy vehicles are considered to experience a hard braking deceleration, with values equal to or greater than 4 m/s^2. Therefore, this scenario simulates a simultaneous hard braking event for all vehicles within the same convoy.

In *Scenario 2* and *Scenario 3*, vehicles of Cat. A are excluded (Table 1), assuming that the braking force produced by the LVs is negligible compared to the others. In *Scenario 2*, a hard braking deceleration value is assigned to all vehicles by sampling from the *PDF* of the maximum deceleration for *HVs*. Conversely, in *Scenario 3*, only the leading vehicle of a convoy (i.e., the first vehicle in the convoy) has a deceleration equal to or greater than 4 m/s^2, while all following vehicles exert a normal braking event with deceleration values ranging from 1 to 7 m/s^2. It is noteworthy that *Scenario 2* corresponds to the most conservative scenario, as it stimulates a hard braking event for all *HVs*. On the other hand, *Scenario 3* represents an intermediate braking event between S*cenario 1* and *Scenario 3*.

PBFM Results

In the following, the *ECDFs* of the resultant braking force $F_{F_{bf,L}}$ generated using Monte Carlo simulations are illustrated. More specifically, Figs. 10–12 show the *ECDFs*

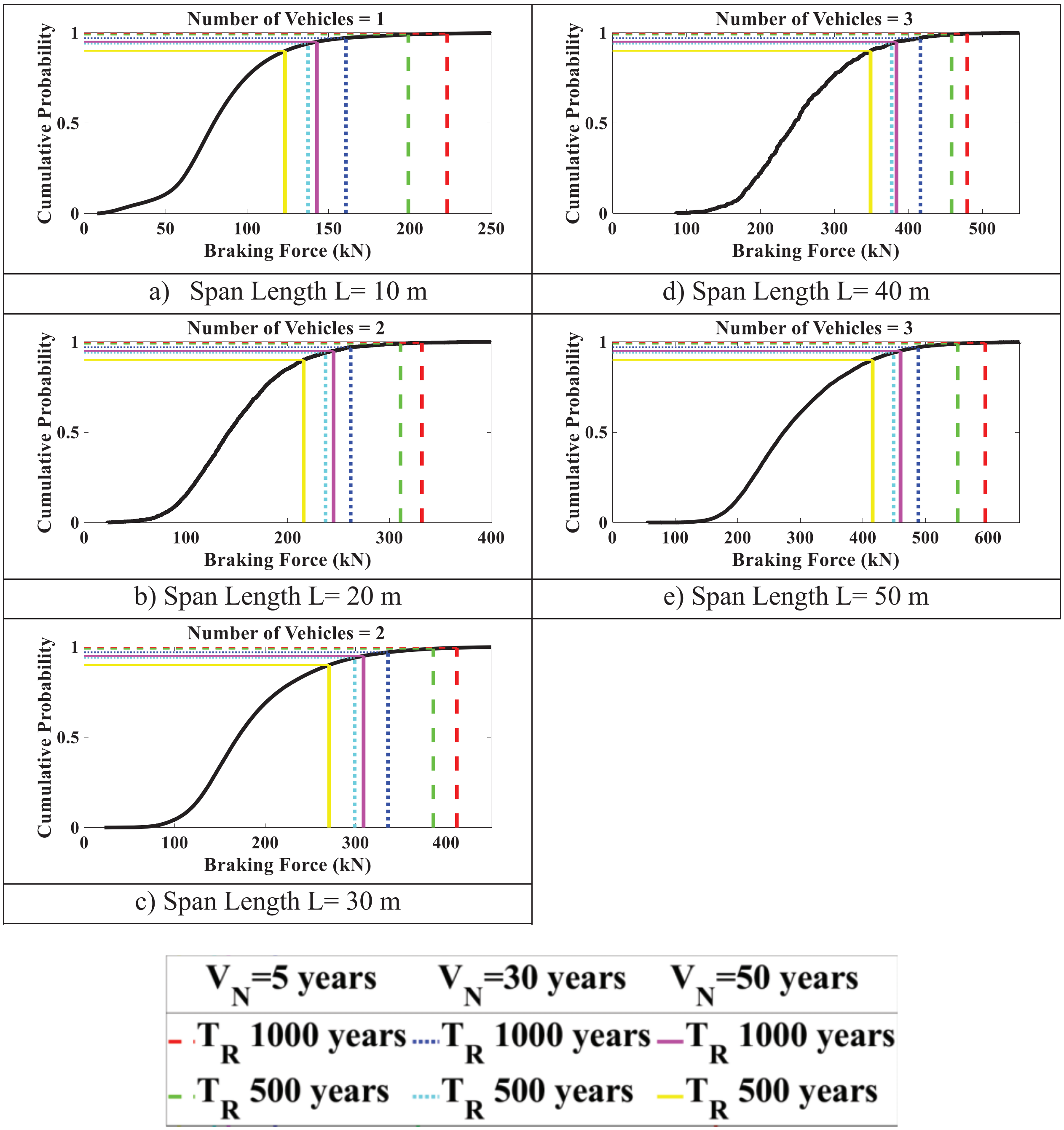

Figure 11. Scenario 2: ECDFs for several span lengths

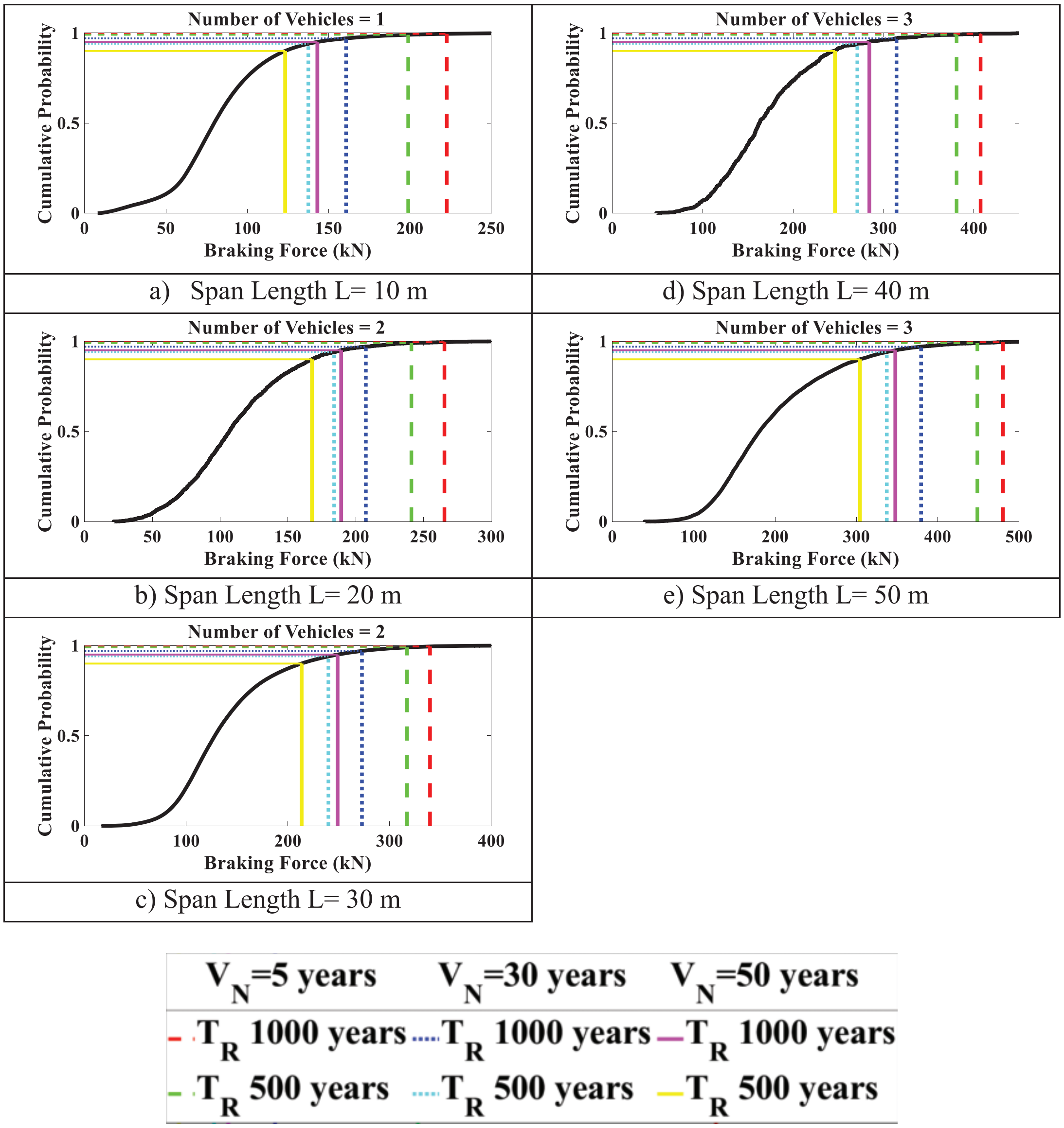

Figure 12. Scenario 3: ECDFs for several span lengths

Table 2. Probability of no-occurrence p for given return period T_R and nominal life V_N (values are in percentage)

	T_R (years)	
V_N (years)	**500**	**1000**
5	99.0	99.5
30	94.0	97.0
50	90.0	95.0

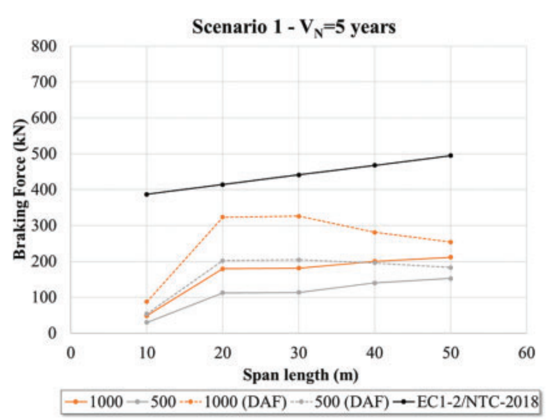

Figure 13. Scenario 1, $V_N = 5$ years

obtained for *Scenario 1*, *Scenario 2*, and *Scenario 3*, respectively. In these graphs, the resultant braking force $F_{bf,L}$ is highlighted for several probabilities p, which are associated (as per Eq. (5)) with predefined return periods T_R (500 and 1000 years) and nominal lives V_N (5, 30, and 50 years). Note that for a given return period T_R, the higher the nominal life V_N, the lower the no-occurrence probability p (Eq. (5) and Table 2). Additionally, in Figs. 10–12, the number of convoy vehicles providing the highest resultant braking force is also indicated. Note that by increasing the span length, more vehicles contribute to the braking force, particularly in Scenario 2 and Scenario 3.

For a given T_R, or equivalently for a given p within V_N, *Scenario 1* (Fig. 10) provides lower resultant braking forces compared to *Scenario 2 and Scenario 3* due to the presence of Cat. A LVs.

Scenario 2 (Fig. 11) provides the highest values of braking forces. Indeed, Cat. A is excluded, and all vehicles within a convoy experience a hard braking deceleration.

Finally, *Scenario 3* (Fig. 12) provides braking forces lower than *Scenario 2*, as Cat. A is also excluded in this case, but only the convoy's leading vehicle is subjected to a deceleration equal to or greater than 4 m/s[2].

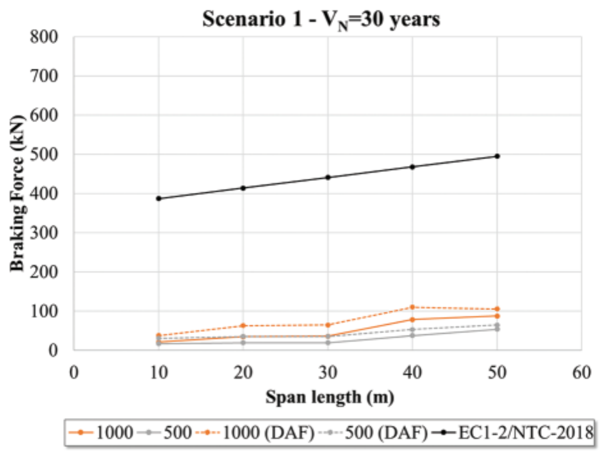

Figure 14. Scenario 1, $V_N = 30$ years

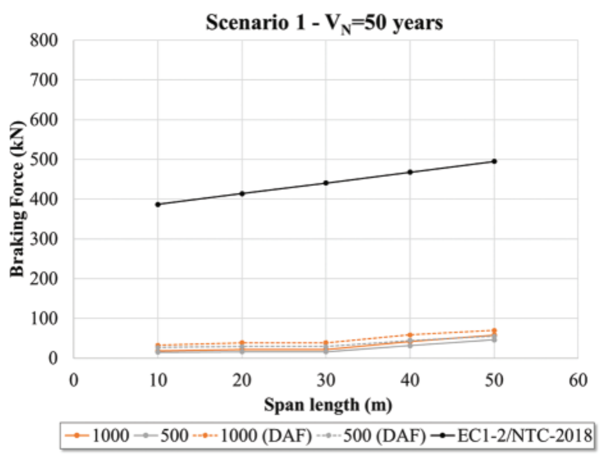

Figure 15. Scenario 1, $V_N = 50$ years

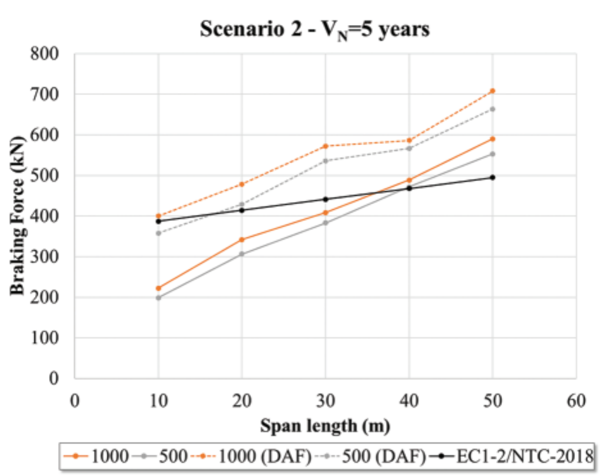

Figure 16. Scenario 2, $V_N = 5$ years

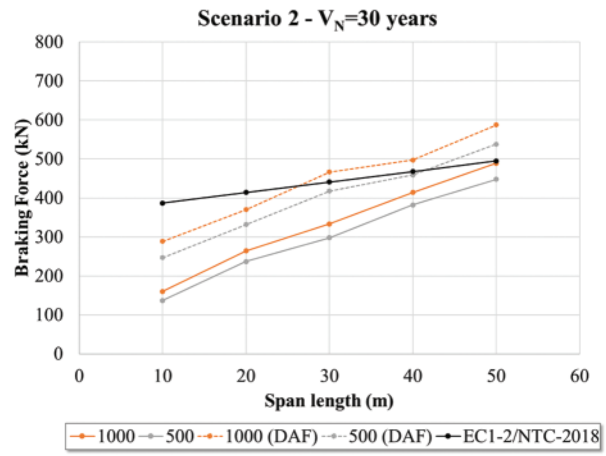

Figure 17. Scenario 2, $V_N = 30$ years

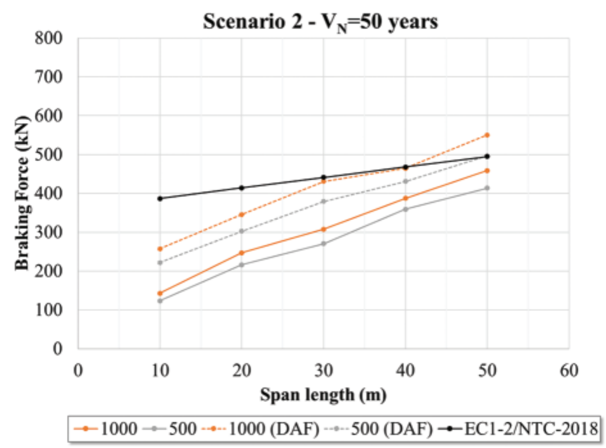

Figure 18. Scenario 2, $V_N = 50$ years

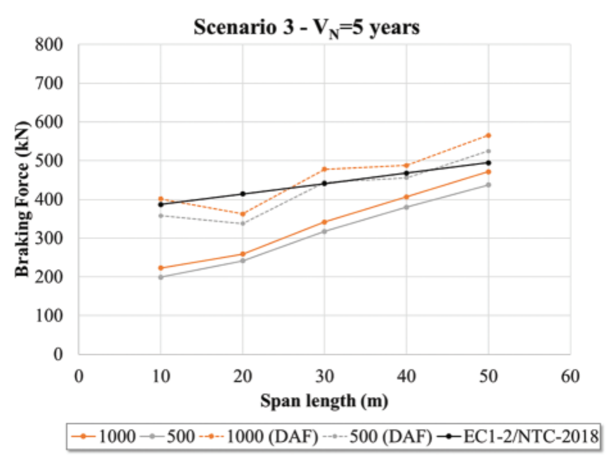

Figure 19. Scenario 3, $V_N = 5$ years

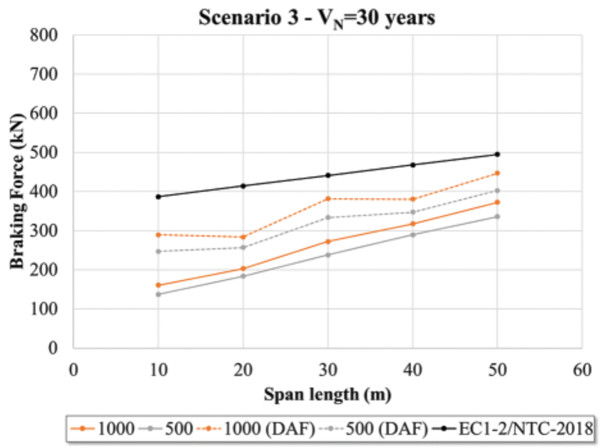

Figure 20. Scenario 3, $V_N = 30$ years

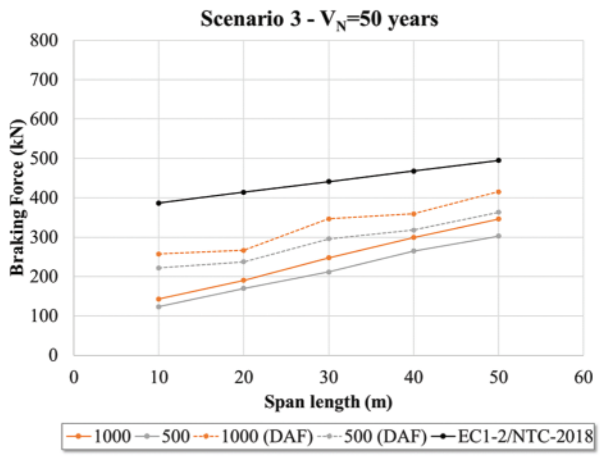

Figure 21. Scenario 3, $V_N = 50$ years

To perform a comparison between the resultant braking force values obtained and those provided by the EC1-2[2] and NTC-2018[4] formulations, the dynamic interaction of braking vehicles and the bridge is taken into account in this study. According to the EC1 background document,[22] by modeling the deck as an *SDOF* system and the braking force as external action, a *DAF* equal to 1.8, 1.4, and 1.2 is obtained for convoys of one, two, and three or more vehicles, respectively. Figs. 13–21 present the resultant braking force for three nominal lives V_N (5, 30, and 50 years) and five return periods T_R (500 and 1000 years) without (continuous lines) and including (dashed lines) the *DAFs* as proposed by the EC1-2.[2] More specifically, Figs. 13–15 refer to *Scenario 1*, Figs. 16–18 to *Scenario 2*, and Figs. 19–21 refer to *Scenario 3*. In these graphs, for each span length, the *DAF* is applied depending on the number of convoy vehicles indicated in Figs. 10–12. Moreover, for completeness, in all figures, the braking force value given by the EC1-2[2] formulation is also plotted (black continuous line).

In general, as one may note, the *PBFM* provides braking forces that, for a given V_N, increase as the span length increases. Also, for a given V_N, the higher T_R, the higher the braking force. However, for a given return period T_R, as V_N increases, the braking force reduces since the probability of no-occurrence *p* (Eq. (5) and Table 2) decreases.

As far as *Scenario 1* is concerned (Figs. 13–15), the braking forces are significantly lower than those provided by EC1-2[2] and NTC-2018.[4] As already discussed, this scenario includes vehicles of Cat. A, whereas EC1-2[2] refers to heavier vehicles, with a single vehicle weighing 40 tons for span lengths less than 25 m, and 30 tons for two and three vehicles for span lengths between 25 and 50 m.

As for *Scenario 2* (Figs. 16–18), for high return period T_R (500 and 1000 years) including DAFs, braking forces may be also higher than the those predicted by EC1-2[2] and NTC-2018[4] for all the three V_N considered (5, 30, and 50 years). This scenario provides the most conservative braking force values.

Finally, in the case of *Scenario 3*, lower braking force values than those in *Scenario 2* are predicted. In this scenario, only for $V_N = 5$ years, including *DAFs* for T_R equal to 500 and 1000 years, braking forces higher than those given by EC1-2[2] and NTC-2018[4] are obtained.

Simplified Equations for PBFM Proposed

Starting from the obtained results, it is possible to derive simplified equations for the proposed *PBFM*, representing a simple tool for designing new bridges and assessing existing ones.

To this end, a numerical regression using the least squares method is applied to the values of resultant braking forces F_{bf} as a function of span length L, return period T_R, and nominal life V_N.

From here on, only braking forces predicted with *Scenario 2*, including *DAFs*, are considered since they provided the most conservative values of braking forces among the

Table 3. Linear regression functions fitting to F_{bf}

F_{bf} (kN)	T_R (years)				
V_N (years)	**30**	**50**	**100**	**500**	**1000**
5	$6.37 \cdot L + 145.52$	$6.82 \cdot L + 163.98$	$7.7 \cdot L + 198.63$	$7.50 \cdot L + 285.68$	$7.23 \cdot L + 332$
30	$4.27 \cdot L + 87.68$	$4.94 \cdot L + 102.83$	$5.71 \cdot L + 124.31$	$7.09 \cdot L + 186.04$	$7.24 \cdot L + 224.84$
50	$3.84 \cdot L + 68.87$	$4.27 \cdot L + 87.68$	$5.19 \cdot L + 108.2$	$6.78 \cdot L + 162.84$	$7.06 \cdot L + 197.99$

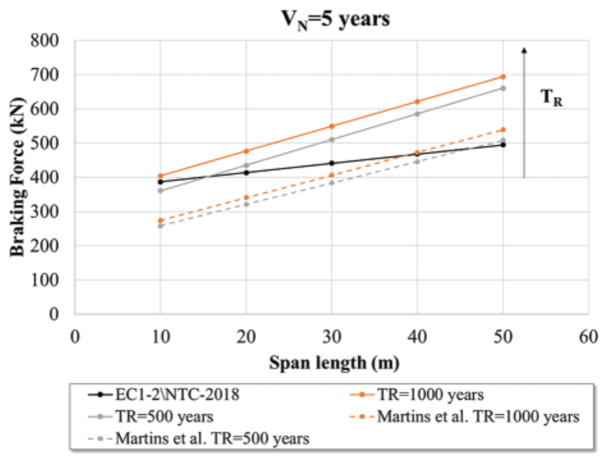

Figure 22. $V_N = 5$ years. Braking force obtained with the linear regression of Table 3

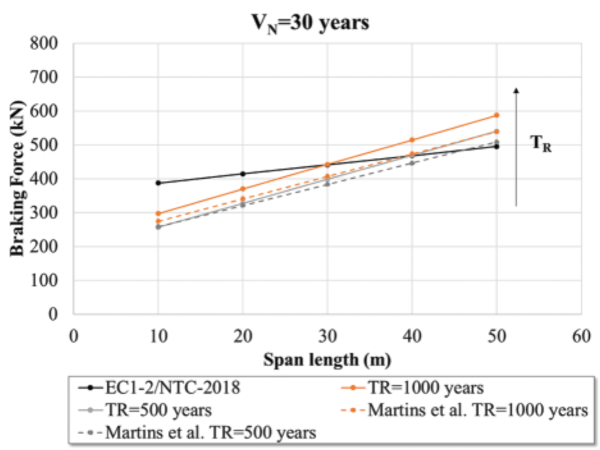

Figure 23. $V_N = 30$ years. Braking force obtained with the linear regression of Table 3

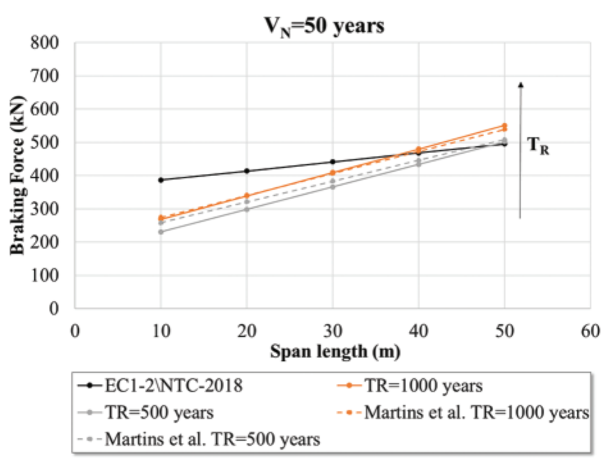

Figure 24. $V_N = 50$ years. Braking force obtained with the linear regression of Table 3

scenarios considered. Table 3 summarizes the resulting linear regressions for predicting the F_{bf} starting from the results Figs. 16–18, obtained by varying T_R and V_N. These regressions are also plotted in Figs. 22–24 by varying V_N, where, for completeness, values obtained with the EC1-2[2]

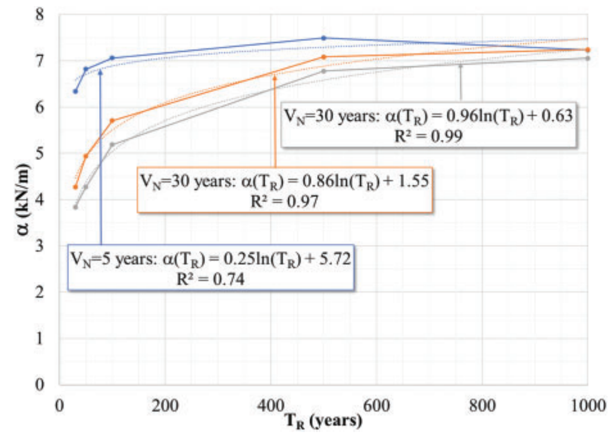

Figure 25. α coefficient

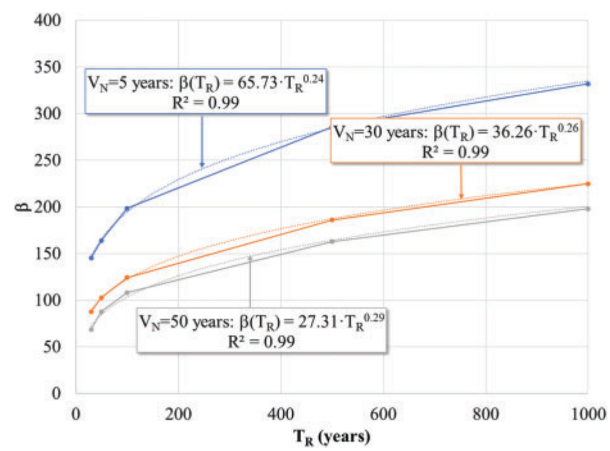

Figure 26. β coefficient

Table 4. Preliminary expressions for α and β coefficients

V_N (years)	$\alpha\,(T_R)$	$\beta\,(T_R)$
5	$\alpha\,(T_R) = 0.25\ln(T_R) + 5.72$	$\beta\,(T_R) = 65.73 \cdot T_R^{0.24}$
30	$\alpha\,(T_R) = 0.86\ln(T_R) + 1.55$	$\beta\,(T_R) = 36.26 \cdot T_R^{0.26}$
50	$\alpha\,(T_R) = 0.96\ln(T_R) + 0.63$	$\beta\,(T_R) = 27.31 \cdot T_R^{0.29}$

and NTC-2018[4] formulations are included. Also, the figures depict the braking force model given by Martins et al.[24], computed for $T_R = 1000$ years, with traffic direction considered equal to 1 and the natural vibration of the bridge structure equal to 3 s.

Then, starting from the linear regressions in Table 3, a design equation for the resultant braking force F_{bf} may be proposed, according to the *PBFM* adopted in this study:

$$F_{bf} = \alpha\,(T_R, V_N) \cdot L + \beta\,(T_R, V_N) \tag{6}$$

where α and β are two coefficient functions that depend on both T_R and V_N, as depicted in Figs. 25 and 26, according to the preliminary expressions summarized in Table 4.

Conclusions

This study proposed a novel PBFM to more accurately estimate braking forces on bridges by incorporating real-world traffic data reflecting the return periods alongside the probabilistic framework of modern design standards. Unlike traditional DBFMs, where the return period is unknown and relies on fixed assumptions about vehicle configurations and braking behaviors, the PBFM utilizes *WIM* data and Monte Carlo simulations to capture the stochastic nature of braking events. By considering key variables such as vehicle weight, length, inter-vehicle distance, and deceleration profiles, this approach determines the value of the braking force that corresponds to a given return period.

The results demonstrate that existing design codes, such as EC1-2,[2] may either overestimate or underestimate braking forces, depending on the bridge span length and return period considered. In particular, for shorter spans, braking forces in EC1-2[2] tend to be more conservative, whereas for longer spans, the proposed probabilistic approach suggests higher braking forces for certain return periods. This discrepancy highlights the limitations of deterministic models in capturing realistic traffic scenarios and underscores the importance of integrating probabilistic methodologies into bridge design and assessment.

The proposed PBFM provides braking force estimates for different return periods (500 and 1000 years) and nominal lives (5, 30, and 50 years), making it adaptable to both existing and newly designed bridges. The study also developed linear regression models to express braking forces as a function of bridge span length and return period, providing engineers with a practical tool for assessing bridge safety under realistic braking loads.

Recommendations for Future Works

Additional traffic parameters, such as road conditions, the number of events expected to occur in a certain period, driver reaction times, and vehicle braking system efficiency, should be evaluated in future studies to further refine braking force estimations. Validating the model using long-term WIM datasets from diverse road sections, including highways and urban roads, could also enrich the dataset, leading to a more accurate model. Investigating the dynamic response of bridges under probabilistic braking forces to enhance structural reliability assessments should also be considered.

Acknowledegments

This work was financially supported by FABRE—Research Consortium for the evaluation and monitoring of bridges, viaducts, and other structures through funds for basic research on "Multi-level safety analysis and monitoring of existing bridges."

Disclaimer

The authors declare no conflict of interest.

Supplemental Materials

Data reported and discussed in this work are available upon request.

References

[1] European Committee for Standardization (CEN), 2002, Eurocode EN, 1990-Basis of structural design.

[2] European Committee for Standardization (CEN). Eurocode EN 1991—Actions on structures. Part 2: Traffic loads on bridges; 2003.

[3] American Association of State Highway and Transportation Officials. *AASHTO LRFD Bridge Design Specifications*. 6th ed.; 2012.

[4] Ministero delle Infrastrutture e dei Trasporti. Norme tecniche per le costruzioni (NTC 2018). Gazzetta Ufficiale della Repubblica Italiana, Serie Generale n. 42, 20 febbraio 2018; 2018.

[5] Jarrahi H, Asadi A, Khatibinia M, Etedali S. Schweizerischer Ingenieur- und Architektenverein SIA (1970), Norm für die Belastungsannahmen, die Inbetriebnahme und Überwachung der Bauten, Norm SIA 160. *J Build Eng*. 2020;27(September 2019):100960. doi:10.1016/j.jobe.2019.100960.

[6] Schweizerischer Ingenieur- und Architektenverein SIA. Einwirkungen auf Tragwerke, Norm SIA 261; 2003.

[7] Standard B. British Standards Institution (1978), BS 5400: steel, concrete and composite bridges. Part 2: specification for loads; 2002 (October).

[8] Martins J, Fénart MA, Feltrin G, Dumont AG, Beyer K. Defining a braking probability to estimate extreme braking forces on road bridges. *12th International Conference on Applications of Statistics and Probability in Civil Engineering, ICASP 2015*; 2015; Published Online. pp. 1–8.

[9] Martins J, Fénart MA, Feltrin G, Dumont AG, Beyer K. Deriving a load model for the braking force on road bridges: comparison between a deterministic and a probabilistic approach. In: *Developments in International Bridge Engineering: Selected Papers from Istanbul Bridge Conference 2014*; 2016; Springer International Publishing.

[10] Breveglieri M, Feltrin G. *Determining Braking Forces on Bridges Using Monitored Traffic Data and Stochastic Simulation*. Vol. 433. Springer Nature Switzerland: LNCE; 2023. doi:10.1007/978-3-031-39117-0_11.

[11] Feltrin G, Breveglieri M. *Dynamic Tests with Hard Braking Heavy Vehicles on a Motorway Bridge*. Vol. 433. Springer Nature Switzerland: LNCE; 2023. doi:10.1007/978-3-031-39117-0_10.

[12] Marshall JD, Anderson JB, Barnes RW, Barr MD, Quinn AJ, Wu H. *Experimental Determination of Braking Force Distribution in Steel Pile Bent Bridges. No. ALDOT 930-928*. Auburn University. Dept. of Civil Engineering; 2020.

[13] Caprani CC. Calibration of a congestion load model for highway bridges using traffic microsimulation. *Struct Eng Int: J Int Assoc Bridge Struct Eng (IABSE)*. 2012;22(3):342–348. doi:10.2749/101686612X13363869853455.

[14] Zhou X, Schmidt F, Toutlemonde F, Jacob B. Applying weigh-in-motion traffic data to reliability based assessment

of bridge structures. In: *ICOSSAR2013, 11th International Conference on Structural Safety & Reliability*; 2013.

[15] OBrien EJ, Bordallo-Ruiz A, Enright B. Lifetime maximum load effects on short-span bridges subject to growing traffic volumes. *Struct Saf*. 2014;50(September):113–122. doi:10.1016/j.strusafe.2014.05.005.

[16] OBrien EJ, O'Connor AJ, Arrigan JE. Procedures for calibrating Eurocode traffic load model 1 for national conditions. *Bridge Maintenance, Saf, Manage, Resilience and Sustain-Proc Sixth Int Conf Bridge Maintenance, Saf Manage*. 2012;20125550(June):2597–2603. doi:10.1201/b12352-397.

[17] Hellebrandt L, Blom CBM, Steenbergen RDJM. Probabilistic traffic load model for short-span city bridges. *Heron*. 2014;59(2–3):147–168.

[18] Aloisio A, Contento A, Alaggio R, Quaranta G. Physics-based models, surrogate models and experimental assessment of the vehicle-bridge interaction in braking conditions. *Mech Syst Signal Process*. 2023;194:110276. doi:10.1016/j.ymssp.2023.110276.

[19] Wang Y, Li S, Wei N. Dynamic response impact of vehicle braking on simply supported beam bridges with corrugated steel webs based on vehicle-bridge coupled vibration analysis. *CMES-Comput Model Eng Sci*. 2024;139(3):3467–3493. doi:10.32604/cmes.2024.046454.

[20] Zhang S, Käding M, Wenner M, Claßen M, Marx S. Structural health monitoring (SHM) on a long semi-integral high-speed railway bridge (HSRB) under different traffic loads. *Eng Struct*. 2025;325:119445. doi:10.1016/j.engstruct.2024.119445.

[21] Dingus TA, Klauer SG, Neale VL, et al. *The 100-car Naturalistic Driving Study, Phase II-Results of the 100-car Field Experiment (No. DOT-HS-810-593)*. United States: Department of Transportation. National Highway Traffic Safety Administration; 2006.

[22] Merzenich G, Sedlacek G. Hintergrundbericht zum Eurocode 1-Teil 3.2: "Verkehrslasten auf Straßenbrücken". *Bundesminister für Verkehr, Abt. Straßenbau, Bonn-Bad Godesberg*. 1995;39(1):98–113. doi:10.1177/1461348419845829.

[23] The MathWorks Inc. MATLAB version: 9.13.0 (R2022b). *The MathWorks Inc*. 2022;142:110–127. doi:10.1016/j.engstruct.2017.03.042.

[24] Martins J, Feltrin G, Beyer K. Updated braking forces for the assessment of road bridges; 2014;(December).

Appendix A

Histogram and PDF of gross mass

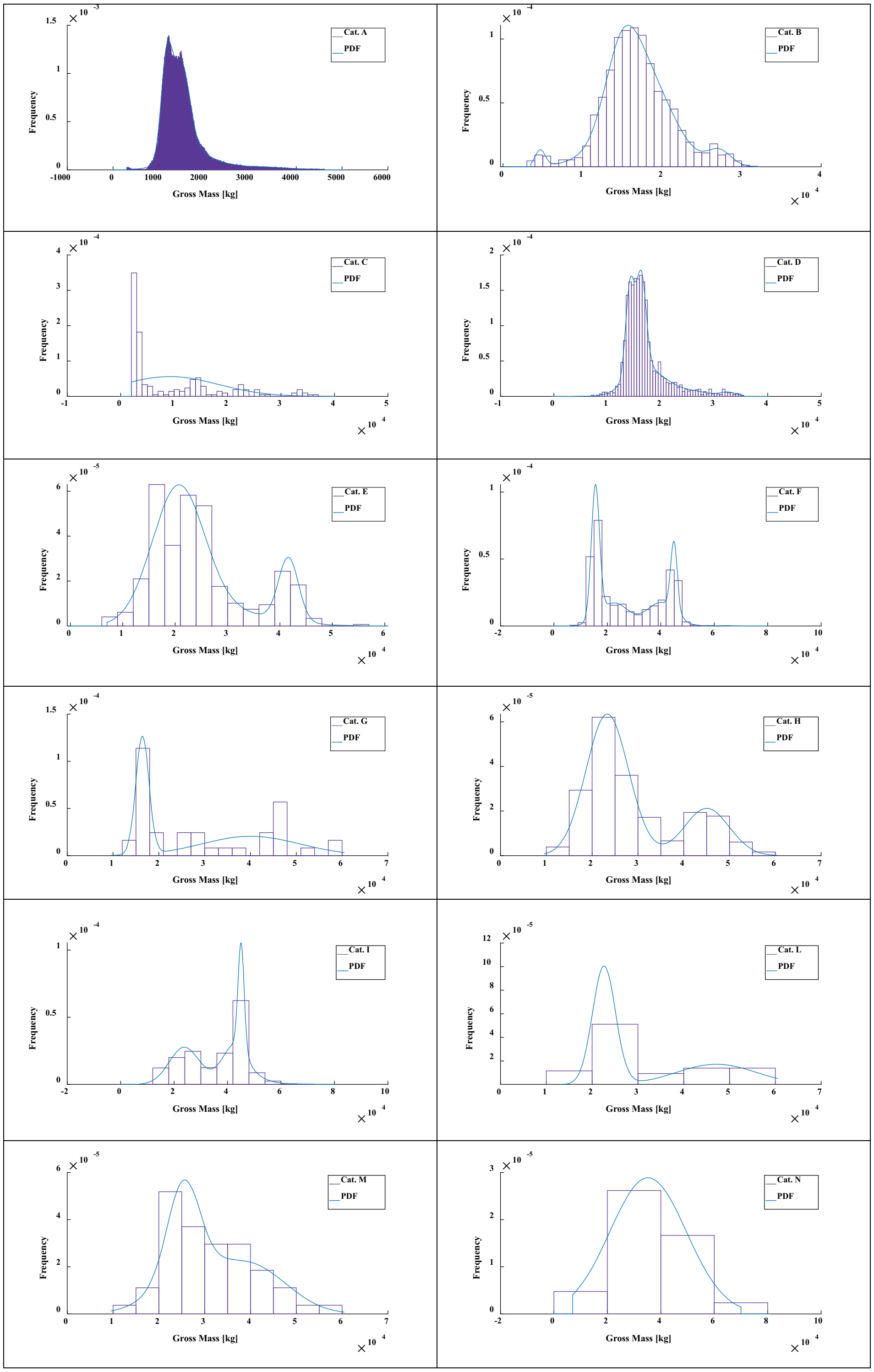

Appendix B

Histogram and PDF of length